

## The analysis of $^{226}\text{Ra}$ in 1-liter seawater by isotope dilution via single-collector sector-field ICP-MS

Lúcia H. Vieira ,\* Walter Geibert, Ingrid Stimac, Dennis Koehler, Michiel M. Rutgers van der Loeff  
Alfred Wegener Institute Helmholtz-Centre for Polar and Marine Research Bremerhaven, Bremerhaven, Germany

### Abstract

The precise determination of radium-226 ( $^{226}\text{Ra}$ ) in environmental samples is challenging due to its low concentration. Seawater typically contains between 0.03 and 0.1  $\text{fg g}^{-1}$   $^{226}\text{Ra}$ . Thus, this work addresses the need for an easy and precise methodology for  $^{226}\text{Ra}$  determination in seawater that may be applied routinely to a large number of samples. For this reason, a new analytical approach has been developed for the quantification of  $^{226}\text{Ra}$  in seawater via inductively coupled plasma mass spectrometry (ICP-MS). Analysis by single collector sector-field ICP-MS was shown to be convenient and reliable for this purpose once potential molecular interferences were excluded by a combination of chemical separation and intermediate mass resolution analysis. The proposed method allows purification of Ra from the sample matrix based on preconcentration by  $\text{MnO}_2$  precipitation, followed by two-column separation using a cation exchange resin and an extraction chromatographic resin. The method can be applied to acidified and unacidified seawater samples. The recovery efficiency for Ra ranged between 90% and 99.8%, with precision of 5%, accuracy of 95.7% to 99.9%, and a detection limit of 0.033  $\text{fg g}^{-1}$  (referring to the original concentration of seawater). The method has been applied to measure  $^{226}\text{Ra}$  concentrations from the North Sea and validated by analyzing samples from the central Arctic (GEOTRACES GN04). Samples from a crossover station (from GEOTRACES GN04 and GEOTRACES GN01 research cruises) were analyzed using alternative methods, and our results are in good agreement with published values.

Radium (Ra) isotopes have been widely applied as tracers and chronometers of processes in the oceans (Knauss et al. 1978; Chung and Craig 1980; Moore and Dymond 1991; Ku and Luo 2008; Charette et al. 2016). Radium is present in seawater at ultratrace levels, with  $^{226}\text{Ra}$  concentrations ranging from 0.0305 to 0.0355  $\text{fg g}^{-1}$  (6.69–7.8 dpm/100 L) in the surface Pacific and Atlantic Oceans (Broecker et al. 1976; Chung and Craig 1980; Sanial et al. 2018), and  $> 0.0683$   $\text{fg g}^{-1}$  ( $> 15$  dpm/100 L) in Southern Ocean surface waters (Vernet et al. 2019). The accurate analysis of such low concentrations of  $^{226}\text{Ra}$  is challenging, as highlighted by an interlaboratory comparison during the GEOTRACES program (Charette et al. 2012).

The capability to measure these low concentrations, on the other hand, is valuable in oceanographic studies. Water masses often have specific  $^{226}\text{Ra}$  signatures that could be better resolved if improved analytical precision was available. In addition, pore-water  $^{226}\text{Ra}$  can provide information about sediment–water exchange (Krishnaswami and Cochran 2008),

but the large sample volumes required for  $^{226}\text{Ra}$  analysis prevent routine measurement in pore water.

Several methods have been applied to determine  $^{226}\text{Ra}$  concentrations in seawater. The majority require preconcentration of Ra from large sample volumes ( $\sim 20$ – $300$  L), and analyses rely on decay counting techniques, which in turn, may require labor-intensive sample preparation or long waiting times for ingrowth and counting. Radiometric techniques include alpha spectrometry (Eikenberg et al. 2001), gamma spectrometry (Michel et al. 1981; Moore 1984; Reyss et al. 1995; van Beek et al. 2010), and by radon emanation (Moore 1969; Key et al. 1979; Roy et al. 2018) or radon-in-air monitor (e.g., RAD-7, DurrIDGE; Kim et al. 2001). The RaDeCC system (Radium Delayed Coincidence Counter), developed by Moore and Arnold (1996) can be used to measure both short-lived (Garcia-Solsona et al. 2008; Moore 2008) and long-lived Ra isotopes such as  $^{226}\text{Ra}$  via  $^{222}\text{Ra}$  ingrowth (Waska et al. 2008; Geibert et al. 2013; Diego-Feliu et al. 2020). More recently, mass spectrometry has been used for  $^{226}\text{Ra}$  determination in seawater, such as thermal ionization mass spectrometry (TIMS) (Cohen and O’Nions 1991; Ghaleb et al. 2004; Ollivier et al. 2008), or multicollector inductively coupled plasma mass spectrometry (MC-ICP-MS) (Foster et al. 2004; Bourquin et al. 2011; Hsieh and Henderson 2011).

\*Correspondence: lucia.lhv@gmail.com

This is an open access article under the terms of the Creative Commons Attribution License, which permits use, distribution and reproduction in any medium, provided the original work is properly cited.

Varga (2008) described the use of sector-field ICP-MS in low salinity water from the Caspian Sea for artificially fortified  $^{226}\text{Ra}$  concentrations. The features and weaknesses of each radiometric and mass spectrometric method have been highlighted in relevant reviews (Lariviere et al. 2006; Hou and Roos 2008; Jia and Jia 2012; Al-Hamarneh and Almasoud 2018; Thakur et al. 2021). Advantages of mass spectrometry compared with conventional decay counting methods are higher precision and fast analysis (a couple of minutes), and smaller sample volumes (< 100 mL vs. 20–1000 L) (Cohen and O’Nions 1991; Larivière et al. 2005; Lagacé et al. 2017; Verlinde et al. 2019). However, although previous methods have efficiently measured  $^{226}\text{Ra}$  by mass spectrometry, there is little consensus on the optimal technique. The widespread application of mass spectrometry for Ra analysis is still limited, no method is routinely applied to a large number of samples, and  $^{226}\text{Ra}$  measurements still rely on decay-counting and emanation techniques.

Analysis of  $^{226}\text{Ra}$  by mass spectrometry may present analytical limitations resulting from instrumental sensitivity and spectral interferences (Lariviere et al. 2006). Barium, for example, behaves chemically like Ra due to its similar ionic potential, and along with other alkaline earth metals in the sample, may cause molecular interferences (e.g.,  $^{88}\text{Sr}^{138}\text{Ba}^+$ ) on the mass spectrometric measurements of  $^{226}\text{Ra}$  (Epov et al. 2003; Larivière et al. 2005; Zoriy et al. 2005; Copia et al. 2015). Foster et al. (2004) showed that the mass difference between the  $^{226}\text{Ra}$  and interference peaks is only 0.2 amu. Chabaux et al. (1994) presented a chromatographic method for Ra purification in volcanic rocks using a combination of AG-50W-X8 and Sr resin. This procedure was subsequently adapted for water matrices (Joannon and Pin 2001; Foster et al. 2004; Sharabi et al. 2010; Lagacé et al. 2017). Although there have been several methodologies for  $^{226}\text{Ra}$  measurement by mass spectrometry in environmental and water samples, few methods have been specifically developed for seawater matrix. Nelson et al. (2014) and Lagacé et al. (2017) showed the importance of considering the effect of sample matrix on Ra recovery for saline waters, as they usually led to poor separation efficiency. Methods for seawater generally include laborious chemical purification involving 3 to 4 column separation procedures, as the column separation steps are reprocessed several times. Although resins are typically reused, these methods may become time-consuming. Therefore, improvements in the Ra chemical purification and instrumental setup would simplify determination of  $^{226}\text{Ra}$  by mass spectrometry.

In addition to sample purification, appropriate instrumentation is crucial for accurate Ra measurements at ultratrace levels. The highest instrumental sensitivity on mass spectrometry is obtained when measurements are performed in low-resolution mode (i.e., FWHM = 300), but this cannot resolve isobaric interferences on  $^{226}\text{Ra}$  (Foster et al. 2004; Lariviere et al. 2006; Leermakers et al. 2009). Yang et al. (2020) showed that polyatomic interferences from Pb and Bi oxides and

hydroxides can only be resolved at a resolution higher than 4000. Verlinde et al. (2019) showed that formation of these interferences strongly depends on the sample introduction system. Isobaric interferences can be resolved in high-resolution mode (FWHM = 10,000), although there is a substantial loss in sensitivity (Varga 2008). In summary, the development of a suitable mass spectrometry method depends on excluding interferences, either by chemical purification or by instrument resolution and the sensitivity of the method. For routine application, any purification method must be simple and rapid.

To solve the sensitivity issue in high-resolution mode, we use a larger sample volume (1000 mL) than previous methods. We present a new analytical approach for an easy and simple determination of natural  $^{226}\text{Ra}$  in acidified and unacidified seawater samples using a single-collector sector-field ICP-MS (ThermoFisher Element 2 ICP-MS). The method is based on the preconcentration of Ra and Ba by  $\text{MnO}_2$  precipitation, followed by chemical separation using a commercially available cation exchange resin and the Triskem Sr-spec resin with subsequent analysis by mass spectrometry. Recovery and repeatability were examined by replicate measurements of  $^{226}\text{Ra}$  concentration in natural seawater from several locations, for which measurements using alternative methods for comparison exist.

The approach used for the method development aimed to minimize the column separation procedures while excluding the effects of interferences on the results. As part of the method development only, we collected and analyzed more fractions than eventually necessary and used advanced mass resolution features of the ICP-MS that are not necessary to apply the methodology.

### Use materials and procedures

All reagents were prepared in deionized water (> 18.2 M $\Omega$  cm; Milli-Q, Millipore). Hydrochloric acid (32%), used to acidify the samples, was purified by single distillation in a quartz sub-boiling still (K. Kürner, Rosenheim, Germany). Nitric acid 65%, ammonia solution 25%, and potassium permanganate ( $\text{KMnO}_4$ ) were purchased from PanReac AppliChem. Manganese (II) chloride tetra-hydrate ( $\text{MnCl}_2 \cdot 4\text{H}_2\text{O}$ ) was purchased from Sigma-Aldrich.

### Spike preparation

A  $^{228}\text{Ra}$  spike was added to the seawater samples before the chemical purification to determine  $^{226}\text{Ra}$  by isotope dilution. The  $^{228}\text{Ra}$  spike was prepared from a commercial 1000 mg L $^{-1}$  Thorium (Th) atomic absorption spectrometry standard using anion exchange resin (Bio-rad AG1 X8). Thorium is retained on this resin in 8 M  $\text{HNO}_3$  while Ra passes it. We first reduced the volume of the  $^{232}\text{Th}$  solution to achieve an acid concentration of about ~ 8 M  $\text{HNO}_3$ , then added ca. 10 g Biorad AG1 X8 resin (batch resin mode) to separate  $^{232}\text{Th}$ . The supernatant

was decanted and passed over 10 mL Biorad AG1 X8 resin equilibrated in 8 M HNO<sub>3</sub> in a 20 mL column (TrisKem). Radium was eluted from the column with 3 CV (column volume) 8 M HNO<sub>3</sub>, then carefully evaporated with heating (avoiding bubbles) to increase the <sup>228</sup>Ra concentration, and taken up in the desired acid concentration by dilution. Thorium-232 was then eluted (after radium) from the resin with 9 M HCl and collected for future use. The resin from the batch mode, containing most of the <sup>232</sup>Th, is kept stored in 8 M HNO<sub>3</sub> for providing access to <sup>228</sup>Ra again after an ingrowth period. The <sup>226</sup>Ra/<sup>228</sup>Ra ratio of the spike will be much lower (improved) on the second separation as <sup>226</sup>Ra ingrowth is much more slowly than <sup>228</sup>Ra. The <sup>228</sup>Ra/<sup>226</sup>Ra ratio of the extracted Ra was 6.03 ± 0.16 (see spike calibration). Radium-228 must be separated from Th to avoid isobaric interference at *m/z* = 228. Although Th-standards can sometimes be purchased as exempt from radiation safety rules, this procedure involves health risks due to the handling of open radioactivity, and it may still be subject to strict regulations. In any case, it should only be performed after a comprehensive risk assessment by trained personnel after making sure that all legal requirements are fulfilled.

### Blanks

Blanks of the chemical procedure, including acid and column contributions, were determined on every ICP-MS measurement and used to correct the final <sup>226</sup>Ra concentrations. Blanks were prepared using 1 liter of deionized water (> 18.2 MΩ cm; Milli-Q, Millipore) spiked with <sup>228</sup>Ra and treated as samples. Seawater blanks were also prepared in order to replicate the sample matrix. For the seawater blanks, 1 liter of North Sea water was gravity filtered three times through a single PVC column loaded with 18 g of MnO<sub>2</sub>-coated fiber (Mn-fiber) at 0.1 L min<sup>-1</sup> to quantitatively remove Ra (Moore 2008; Charette et al. 2012). No differences in <sup>226</sup>Ra counts and <sup>228</sup>Ra/<sup>226</sup>Ra ratios were observed between MilliQ and seawater blanks.

### Chemical purification

One liter of seawater was acidified to pH 1.0 using distilled HCl (32%). After gravimetric addition of the <sup>228</sup>Ra spike solution (~ 100 fg or ~ 60 dpm), the sample was stirred continuously on a stirrer plate with a Teflon-covered magnetic stir bar. In the next stage, Ra preconcentration was performed using MnO<sub>2</sub> coprecipitation following a modified method of Ghaleb et al. (2004). A 1 mL of 0.25 M KMnO<sub>4</sub> solution was added to the (acidified and unacidified) samples, and the pH was adjusted to 8.5–9 by adding Ammonia Solution 25%. The pH was checked using pH strips (Carl Roth™) and a pH meter when necessary. Next, 1 mL of 0.5 M MnCl<sub>2</sub>·4H<sub>2</sub>O was added; at this stage, Mn<sup>2+</sup> is oxidized to Mn<sup>4+</sup>, forming insoluble MnO<sub>2</sub>. The solution was then stirred for 2 h at 80°C and allowed to stand overnight.

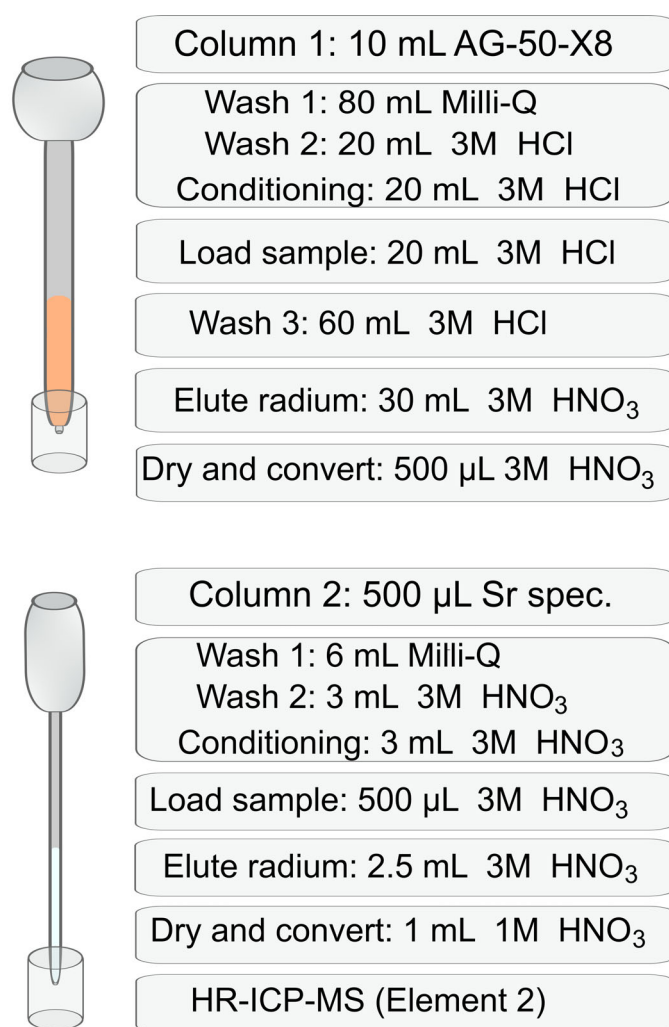


**Fig 1.** Schematic diagram for cation exchange separation and purification of Ra from seawater.

The supernatant was then discarded, and the precipitate recovered by centrifugation, washed twice with Milli-Q, and transferred into a 50 mL Teflon™ beaker. The precipitate was dissolved in 20 mL 6 M HCl, and few drops (3–4) of 1 M hydroxylamine were added for a complete reduction of MnO<sub>2</sub> to Mn<sup>2+</sup>. The solution was brought to dryness and taken up in 20 mL 3 M HCl, ready for the column separation procedure.

### Column separation

Radium purification was performed by cation exchange chromatography using commercially available columns (20 mL; Triskem Int., AC-20E-20M), Bio-rad AG-50-X8 (200–400 mesh) hydrogen form resin (biotechnology and analytical grades), and Sr-spec resin (TrisKem Int., SR-B25-A). A 20 mL column was filled with 10 mL of AG-50-X8 resin (Fig. 1), to separate elements such as Mn, Ca, and Sr from the Ba-Ra fractions (Fig. 2). The second extraction was performed using a 1 mL Thermo Scientific Samco Transfer Pipette filled with

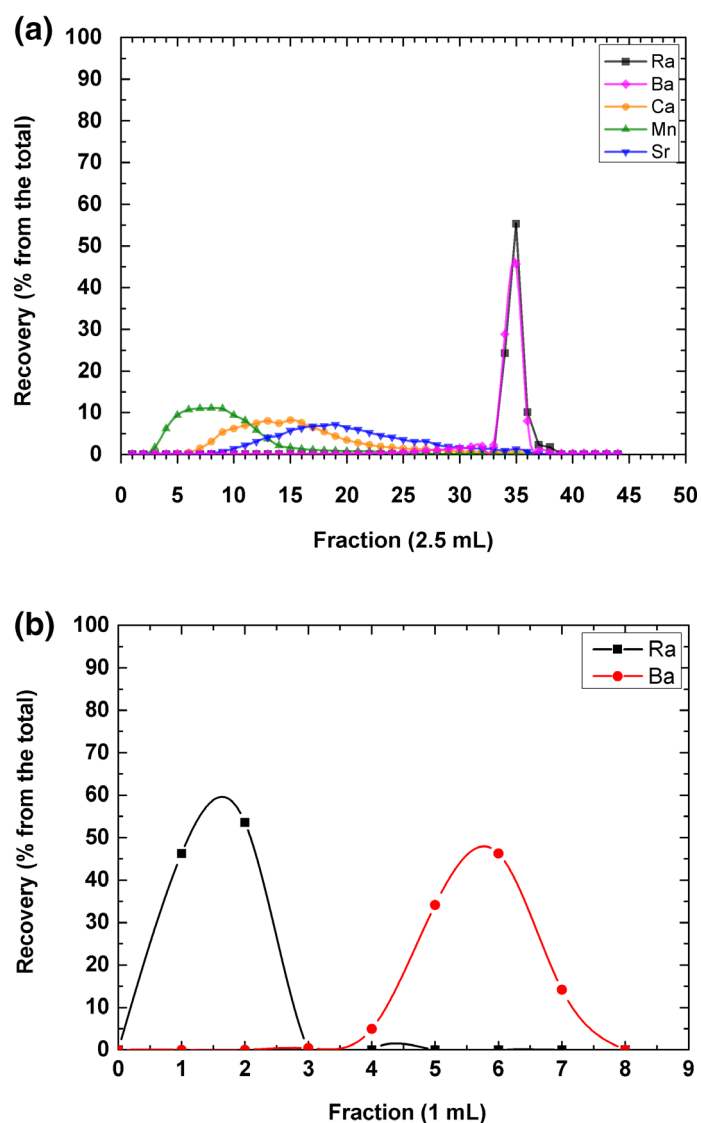


**Fig 2.** (a) Elution curve for Mn, Ca, Sr, Ba, and Ra on the first cation exchange column (10 mL AG-50W-X8). (b) Elution curve for Ba and Ra on the Sr spec column. Radium recovery was determined by gamma spectrometry, while Mn, Ca, Sr, and Ba recoveries were obtained by ICP-OES.

500  $\mu\text{L}$  of Sr resin to separate radium isotopes from barium following a slightly modified method of Hsieh and Henderson (2011).

We collected the eluted fraction from the columns in small increments to assess the separation of potentially interfering elements. The AG-50-X8 cation exchange resin was thoroughly rinsed with Milli-Q and 3 M HCl before conditioning to remove Sr and Pb (Varga 2008). The first column was preconditioned with 20 mL of 3 M HCl, and samples were loaded in 20 mL 3 M HCl (fractions 1–8). Next, the column was washed with 60 mL of 3 M HCl to remove Mn, Ca, and Sr (fractions 9–32). Ra and Ba were then eluted in 30 mL 5 M  $\text{HNO}_3$  at roughly 2  $\text{mL min}^{-1}$  (fractions 33–44). Radium was

detected in fractions 34–38 (Fig. 2a), but all elution fractions (33–44) were combined, brought to dryness, and converted into 500  $\mu\text{L}$  3 M  $\text{HNO}_3$ , which was then loaded onto the second column preconditioned with 6 mL 3 M  $\text{HNO}_3$ . Radium was eluted with 2.5 mL 3 M  $\text{HNO}_3$  at roughly 0.3  $\text{mL min}^{-1}$ , evaporated, and taken up in 1 mL 1 M  $\text{HNO}_3$  for analysis (Fig. 1). A fresh batch of resins was used for each sample.

For column calibration purposes, the eluate from the columns was collected in fractions of 2.5 mL (from column 1) and 1 mL (from column 2). A 200  $\mu\text{L}$  from each fraction was taken, added into 3.8 mL 1 M  $\text{HNO}_3$ , and Mn, Ca, Sr, and Ba subsequently measured by Inductively Coupled Plasma Optical Emission Spectrometry (Thermo Scientific, ThermoFisher iCap, ICP-OES; Fig. 2).

### Mass spectrometry

Analyses of  $^{226}\text{Ra}$  were performed using a ThermoFisher Element 2 sector field inductively coupled plasma mass spectrometry (HR-ICP-MS) at the Alfred Wegener Institute (AWI), Germany. The ICP-MS was equipped with a “flattop peak medium resolution kit” that replaces the usual  $R = 10,000$  resolution with a resolution of  $R = 2000$ . It produces flat top peaks that allow the separation of typical radium interferants but provide better sensitivity than medium resolution. The mass resolution is between typical “low” ( $R = 300$ ) and “medium” ( $R = 4000$ ), and is referred to here as “intermediate” resolution (IR). This feature was used for the method development, but it is not essential for applying the method described here. The ICP-MS method for analysis in IR also included a full scan in low resolution to examine peak shape and check any interferences that would affect the ratio. All data were therefore acquired in low ( $R = 300$ ) and intermediate resolutions ( $R = 2000$ ). We used the  $^{228}\text{Ra}/^{226}\text{Ra}$  ratios provided by the low-resolution (LR) analysis after ensuring that interferences were not present on the IR peak spectrum. Figure 3 shows the spectra of a sample analyzed in IR and LR. Radium-226 was determined by isotope dilution.

Mass regions measured for  $^{226}\text{Ra}$  and  $^{228}\text{Ra}$  were 225.7466 to 226.3033 and 227.4799 to 228.3122, respectively. The instrument was tuned before each measurement for maximum sensitivity and stability using a solution of Indium (In) and Uranium (U) ( $\text{RSD} < 2\%$ ). Parameters such as torch position, cool gas, auxiliary gas, sample gas, lenses, and RF power were optimized before each ICP-MS run. An Apex-IR desolvating nebulizer (ESI) was used to minimize formation of molecular interferences (Lariviere et al. 2006) and increase sensitivity. Verlinde et al. (2019) demonstrated the superior performance of the Element 2 ICP-MS in combination with an Apex-Q compared to other ICP-MS instruments, presenting a detection limit as low as 0.024  $\text{fg g}^{-1}$ . Typical sensitivities of our system in this setup are around 12 million  $\text{cps } \mu\text{g}^{-1} \text{L}^{-1}$  in low resolution. The sampling cone (X8) and skimmer cone (standard) were made of nickel. Mass bias was monitored at mass 238 and 235 with a natural U standard solution (0.2  $\mu\text{g L}^{-1}$  U).

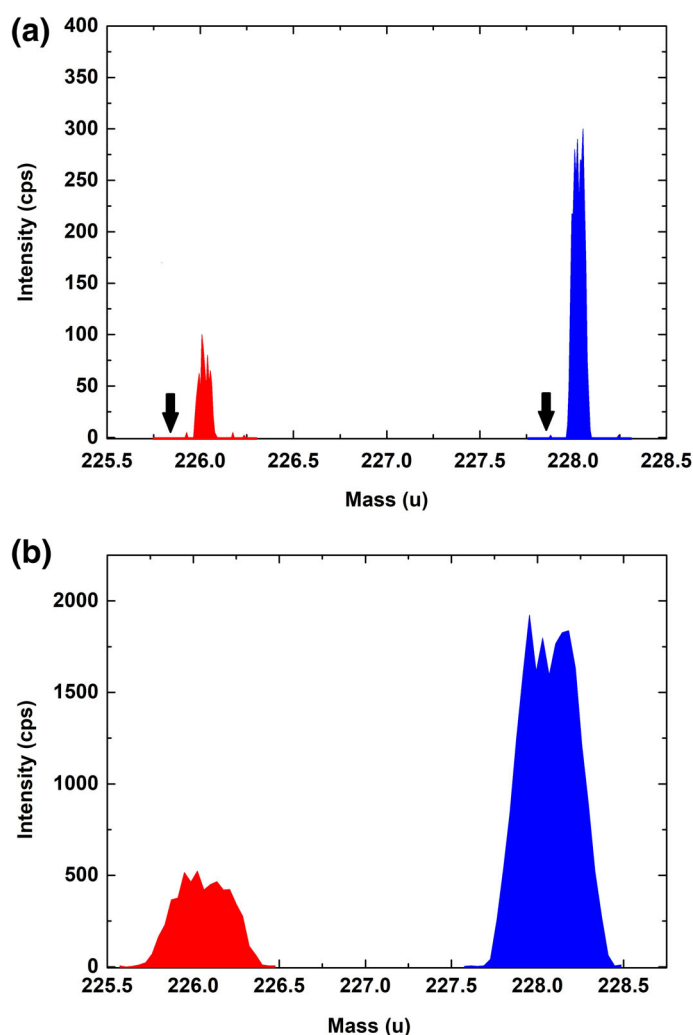


**Fig 3.** (a) Intermediate resolution mass spectrum (flat-topped peak) of a North Sea sample. Arrows represent the location of potential interferences in case they were present. (b) Full scan in low-resolution of the same sample.

### Assessment

Radium samples are typically acidified after collection, but unacidified samples were also tested ( $n = 3$ ) as an alternative for sample preparation on board before analysis in a land-based laboratory. The Mn-precipitation step, can be performed directly after sample collection, and the sample volume reduced from 1 L to 5–10 mL. No difference was observed between acidified and unacidified samples during the whole procedure, except adjustment of the pH before coprecipitation, in which case less ammonia solution is required for unacidified samples (3–4 drops vs. 30–150 drops to acidified samples).

The coprecipitation method used here allows the incorporation of Ba and Ra on  $\text{MnO}_2$  and aids the partial removal of chemical elements from the solution which are not of interest,

such as Ca and Sr (Ghaleb et al. 2004). Coprecipitation of Ra on  $\text{MnO}_2$  is pH sensitive, so adjustment from pH 1 to 8.5 should be carefully performed. Coprecipitation is thought to occur by surface sorption and high pH increases the negative charge of the  $\text{MnO}_2$  and improves its capacity to adsorb radium (Moon et al. 2003). However, pH should not exceed 9, as coprecipitation of magnesium (Mg) may occur. Strelow (1984) and Bohlin et al. (2018) have shown that the affinity of Mg to the cation exchange resin (AG MP-50) decreases with increasing HCl concentration. Nonetheless, the presence of Mg in the sample can result in non-spectral interferences during the determination of  $^{226}\text{Ra}$  by ICP-MS (Larivière et al. 2005) and should be avoided.

After redissolution of the precipitate, two columns were used to extract Ra. Radium and Ba were well separated from Mn, Ca, and Sr after the cation exchange column separation (Fig. 2a). The thin and long column 2 produced effective peak separation of Ra and Ba (Fig. 2b). Potential molecular interference caused by  $^{88}\text{Sr}^{138}\text{Ba}$  on the  $^{226}\text{Ra}$  analysis by HR-ICP-MS is considerable if the concentrations of Sr and Ba exceed 1 and  $10 \mu\text{g L}^{-1}$ , respectively (Park et al. 1999). In our study, the concentration of Ba was around  $1.5 \pm 0.1 \mu\text{g L}^{-1}$ , and Sr was undetectable in the fractions where Ra was eluted (Fig. 2b). Furthermore, no interferences were observed on the radium peaks analyzed in intermediate mass resolution (Fig. 3).

### $^{228}\text{Ra}$ spike calibration

The  $^{228}\text{Ra}$  concentration of the spike (reference date: 10 July 2020) was determined by isotope dilution via ICP-MS measurements using a calibrated  $^{226}\text{Ra}$  standard ( $\sim 240,000 \text{ fg g}^{-1}$  on 13 August 2020). Increasing amounts of  $^{226}\text{Ra}$  standard solution (in the range from 0 to 24,050 fg) were added gravimetrically to  $^{228}\text{Ra}$ -spiked North Sea samples, allowing to calculate  $^{228}\text{Ra}$  concentration of  $255 \pm 4 \text{ fg g}^{-1}$  in the  $^{228}\text{Ra}$  spike (standard deviation from the average) (Fig. 4). The spike  $^{228}\text{Ra}/^{226}\text{Ra}$  ratio was  $6.03 \pm 0.16$ . The  $^{226}\text{Ra}$  contribution from the spike was corrected for every measurement. The  $^{226}\text{Ra}$  standard was made by gravimetric dilution of a NIST standard, kept sealed with Parafilm in a teflon bottle, and corrected for decay since the certified date. A small amount of evaporation could have occurred, but repeated comparisons with reference materials (e.g., DL1-A) and cross calibrations with other laboratories (Woods Hole Laboratory, University of South Carolina) confirm that this is negligible.

### Recovery, accuracy, and repeatability

Column eluate fractions were analyzed by gamma spectrometry, and column recoveries determined relative to the  $^{228}\text{Ra}$  spike. The  $^{228}\text{Ac}$  peaks (338 and 911 keV) were used to determine  $^{228}\text{Ra}$ , and gamma analysis was performed 2 d after the column separation in order to allow the ingrowth of  $^{228}\text{Ac}$  (half-life 6.15 h). Total radium recovery ranged between 90% and 99.8% (average 93%,  $n = 13$ ). We observed that up to 10% Ra is lost in the precipitation step. Bourquin et al. (2011)



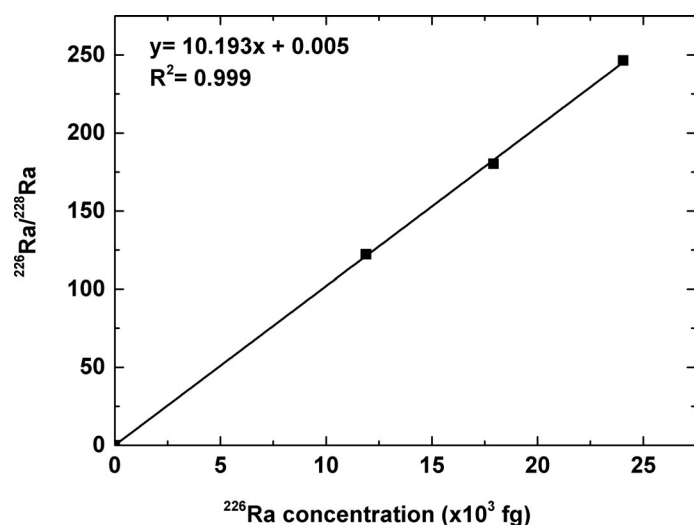


**Fig 4.** Standard addition curve for the calibration of  $^{228}\text{Ra}$  spike.

report that the preconcentration using  $\text{MnO}_2$  coprecipitation technique seems to improve the yield of Ra recovery compared to other techniques.

We tested Bio-rad AG-50-X8 (200–400 mesh) resins of biotechnology and analytical grade and observed no difference on Ra recovery. However, the analytical grade seems to contain higher levels of Sr and may need to be washed with more 3 M HCl before the conditioning and the Ra–Ba elution steps from column 1 (Fig. 1).

Further tests were performed to reduce the amount of AG-50-X8 resin on the first column separation. Extraction recoveries of  $90\% \pm 1\%$  ( $n = 3$ ) were obtained for 5 mL of resin in a 5 mL column (Triskem Int). The smaller columns require 20 mL 3 M HCl for preconditioning, loading of 10 mL sample, washing with 30 mL 3 M HCl, and elution with 20 mL 5 M  $\text{HNO}_3$ .

The precision of the method was assessed by analyzing six replicates of North Sea samples. Replicate measurements of  $^{226}\text{Ra}$  are shown in Fig. 5. The average value of the  $^{226}\text{Ra}$  concentration is  $0.049 \pm 0.003 \text{ fg g}^{-1}$  ( $10.7 \pm 0.49 \text{ dpm}/100 \text{ L}$ ) ( $1\sigma$  uncertainty).

Accuracy of 95.7% to 99.9% was determined using the standard addition method by adding an increasing amount of  $^{226}\text{Ra}$  spike to North Sea blank samples, treated and analyzed as natural samples. Final  $^{226}\text{Ra}$  concentrations in the standard addition samples were compared with the amount of  $^{226}\text{Ra}$  spike added to these samples prior to the precipitation step. Accuracy was expressed as a percentage recovery: measured  $^{226}\text{Ra}$  value/added  $^{226}\text{Ra}$  (spike). In the absence of a certified  $^{228}\text{Ra}$  spike, the accuracy of the  $^{226}\text{Ra}$  measurements is hard to confirm. This was checked with a  $^{228}\text{Ra}$  spike ( $1711 \pm 42 \text{ fg g}^{-1}$ ) that had been cross-calibrated by gamma spectrometry and HR-ICP-MS. This spike can be called here “spike 2” to differentiate from that used on the method development described in the Spike Calibration section.

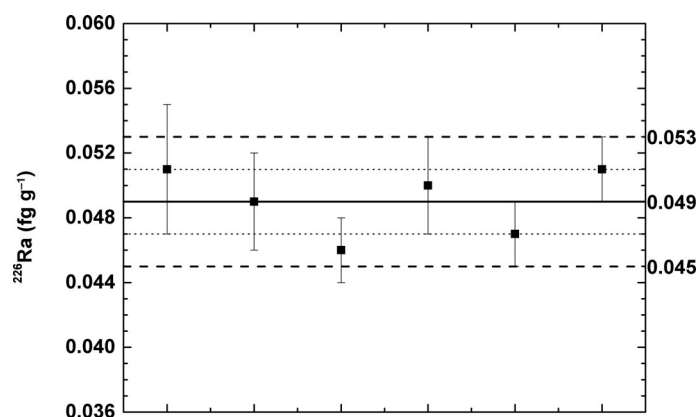


**Fig 5.** Replicate measurement of  $^{226}\text{Ra}$  by single-collector sector-field ICP-MS. Error bars represent the uncertainties on the measurement; short dashed lines and dashed lines represent  $1\sigma$  and  $2\sigma$ , respectively.

The instrumental detection limit of  $0.033 \text{ fg g}^{-1}$  was calculated as three times the standard deviation of the procedural blanks described above.

#### Method evaluation

As an application of the proposed method,  $^{226}\text{Ra}$  was determined in a depth profile from the Arctic Ocean collected during the GEOTRACES section GN04 (Fig. 6).

In the framework of the GEOTRACES program, two research cruises took place in 2015 to the central Arctic: GEOTRACES - GN04 on RV Polarstern (expedition PS94) and GEOTRACES - GN01 on USCGC Healy (expedition HLY1502). At the crossover station, that is, PS94 Sta. 101 and HLY1502 Sta. 30, water column samples were collected for Ra analysis with in situ pumps (ISP) equipped with  $\text{MnO}_2$ -coated cartridges (Mn-cartridges) (Henderson et al. 2013). Radium extraction efficiencies of the Mn-cartridges on the GEOTRACES - GN01 cruise were determined using 15–20 L discrete samples (collected at corresponding ISP depths) that were filtered through Mn-fibers (Kipp et al. 2019). The  $^{226}\text{Ra}$  activities on the fibers were then compared to those determined on the corresponding cartridges. During the GEOTRACES - GN04 (PS94), two cartridges were placed in series on some pumps at selected stations. The Mn-cartridge extraction efficiencies from the GN04 cruise were estimated from the relative activity on the two cartridges (Rutgers van der Loeff et al. 2018). Small-volume samples (1 liter) were collected at Sta. 101 during the PS94 expedition for analysis of  $^{226}\text{Ra}$  by mass spectrometry. Six of these samples analyzed by the proposed method are in good agreement with GEOTRACES - GN01 (Fig. 6), which implies that the offset observed on the  $^{226}\text{Ra}$  distribution in deep waters from the GEOTRACES - GN04 is likely due to overestimation of their constant cartridge efficiency.

Samples from the North Sea had a  $^{226}\text{Ra}$  concentration of  $0.049 \pm 0.003 \text{ fg g}^{-1}$  (Fig. 5). Radium isotopes have been

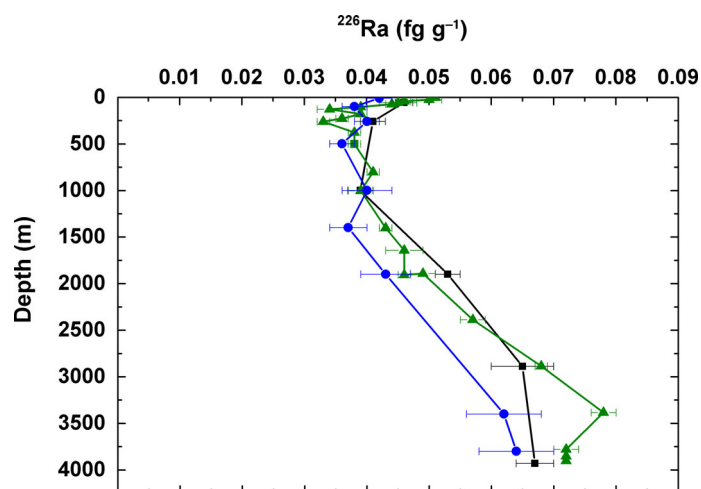


**Fig 6.** Vertical profiles of  $^{226}\text{Ra}$  at the crossover station from GEOTRACES GN01 (triangle), GEOTRACES GN04 (Rutgers van der Loeff et al. 2018; circle) and GEOTRACES GN04 (this study; square).

already applied as tracers of land-ocean exchange and pore water fluxes in the North Sea (Moore et al. 2011; Schmidt et al. 2011; Burt et al. 2014). Nonetheless, there are still limited data on  $^{226}\text{Ra}$  activities in seawater in this region. Schmidt et al. (2011) reported  $^{226}\text{Ra}$  activities ranging from 0.037 to 0.075  $\text{fg g}^{-1}$  (8.2–16.5 dpm/100 L) between the coastal and open ocean region, which are in agreement with our data from the North Sea (Fig. 5).

## Discussion

The proposed analytical method has been developed and successfully applied to acidified and unacidified seawater samples. For measurement of Ra isotopes by mass spectrometry, good separation of Ra from other alkaline earth elements is crucial to avoid mass interferences. The current method does this successfully for analysis by single-collector sector field ICP-MS.  $^{228}\text{Ra}$  from the spike was separated from its daughter  $^{228}\text{Th}$ , which can form isobaric interference on  $m/z = 228$ . Radium was also completely separated from the other alkaline earth elements (e.g., Ca, Sr, and Ba). The presence of  $^{88}\text{Sr}^{138}\text{Ba}$  is thought to be one of the major contributors to molecular interferences. In our study, Sr was undetectable after the final separation so that residual Ba is irrelevant. Nonetheless, Ba concentration ( $1.5 \mu\text{g L}^{-1}$ ) was almost tenfold lower than the level that may cause interferences ( $10 \mu\text{g L}^{-1}$ ). Furthermore, low concentrations of Ba avoid salt accumulation on the sampler and skimmer cones (Foster et al. 2004).

Several other polyatomic interferences have been identified on the  $^{226}\text{Ra}$  analysis by mass spectrometry, such as those from Sr, tungsten (W), platinum (Pt), mercury (Hg), lead (Pb), bismuth (Bi), and thallium (Tl), that is,  $^{86}\text{Sr}^{140}\text{Ce}$ ,  $^{87}\text{Sr}^{139}\text{La}$ ,  $^{186}\text{W}^{40}\text{Ca}$ ,  $^{186}\text{W}^{40}\text{Ar}$ ,  $^{194}\text{Pt}^{16}\text{O}_2$ ,  $^{199}\text{Hg}^{27}\text{Al}$ ,  $^{202}\text{Hg}^{24}\text{Mg}$ ,  $^{208}\text{Pb}^{17}\text{O}^1\text{H}$ ,  $^{208}\text{Pb}^{18}\text{O}$ ,  $^{208}\text{Pb}^{16}\text{O}^1\text{H}_2$ ,  $^{209}\text{Bi}^{16}\text{O}^1\text{H}$ ,  $^{209}\text{Bi}^{17}\text{O}$ , and

$^{203}\text{Tl}^{23}\text{Na}$  (Park et al. 1999; Epov et al. 2003; Lariviere et al. 2006). However, no interference was observed on the  $^{226}\text{Ra}$  and  $^{228}\text{Ra}$  spectrum from the HR-ICP-MS analysis (Fig. 3).

This study used an intermediate resolution of 2000 to demonstrate the absence of these interferences, in contrast with other studies that used low-resolution mode for HR-ICP-MS measurement of Ra in environmental samples (Park et al. 1999; Sharabi et al. 2010; Copia et al. 2015). Although the sensitivity in low-resolution is almost 10 times higher than in high/intermediate resolution, possible molecular interferences may not be well separated from the  $^{226}\text{Ra}$  peak resulting in incorrect values at  $\text{fg g}^{-1}$  levels of Ra. The current method gives flat-topped peaks that allow the complete mass-spectrometric separation of potential interferants. In a similar study, Varga 2008 used medium resolution ( $R = 4000$ ) on a double-focusing sector-field inductively coupled plasma mass spectrometry (HR-ICP-MS) but used artificially enriched  $^{226}\text{Ra}$  in low salinity Caspian Sea water to reach the required count rates. In comparison, we used seawater from the North Sea and the Arctic Ocean with natural  $^{226}\text{Ra}$  concentrations and achieve sufficient sensitivity by increasing the sample volume from 10–300 to 1000 mL (see Table 2).

Recovery of the method ranged between 90% and 99.8% and is similar to that reported by Foster et al. (2004) and Bourquin et al. (2011) (~90%) (MC-ICP-MS), but higher than that reported by Varga (2008) (ICP-SFMS) and Ghaleb et al. (2004) (73%–94%) (TIMS). The 5% precision of the current method is similar to that found by Bourquin et al. (2011) (2.5%–6.6%) and Foster et al. (2004). Hsieh and Henderson (2011) reported a precision of 2% by MC-ICP-MS. The uncertainties reported here may be slightly higher than those reported in other studies, but includes error propagation from the concentrations and isotope ratios of the  $^{228}\text{Ra}$  spike and blanks. A  $^{228}\text{Ra}$  spike with no trace of  $^{226}\text{Ra}$  would be ideal to obtain a better background and low uncertainties. However, no such commercial  $^{228}\text{Ra}$  spike is available, and manually produced spike (in small batches) has variable  $^{228}\text{Ra}/^{226}\text{Ra}$  ratios. Although MC-ICP-MS and TIMS may achieve a lower detector limit and background, these instruments are not readily available in most laboratories, whereas single-sector field ICP-MS is currently common and widely used.

The detection limit of 0.033  $\text{fg g}^{-1}$  (referring to the original seawater concentration) is comparable to radiochemical methods such as alpha spectrometry or Rn emanation. However, the proposed method avoids long waiting periods for ingrowth and counting, and requires significantly smaller sample amounts (Table 2). In addition, the current method has better precision than gamma spectrometry. Smaller sample amounts also open new possibilities for pore-water analyses. The proposed method was successfully applied in 60–80 mL of sediment pore water from the Pacific Ocean, and will be detailed in a separate publication.

Further reduction of detection limits for  $^{226}\text{Ra}$  will require a commercially available  $^{228}\text{Ra}$  spike with a low and certified

**Table 1.** Data acquisition parameters for the detection of  $^{226}\text{Ra}$  and  $^{228}\text{Ra}$  by element 2 ICP-MS. Note that the values for “mass window” and “samples per peak” for R = 2000 are misleading since the instrument software assumes the R = 10,000 slit to be present, leading to a factor of five difference between the apparent and the actual values.

Instrumental parameters	Method: Full peak scan		Method: Peak hopping ratio
	Resolution	300	2000
Number of runs	1	2	5
Number of passes	1	1	3
Mass window	125	2500	5
Mass magnet	226.025	226.025	226.025
Settling time	0.001	0.001	0.001
Sample time	0.3	0.2	0.25
Samples per peak	20	3	300
Segment duration	7.5	15	3.75
Search window	100	100	0
Integration window	100	60	5
Scan type	EScan	EScan	EScan
Detection mode	Counting	Counting	Counting
Integration type	Average	Average	Average
Acquisition time	16 s	1 min 01 s	1 min 53 s

amount of  $^{226}\text{Ra}$ . Furthermore, the sensitivity of the ICP-MS instrument still plays a crucial role, as a higher sensitivity translates to longer acquisition times.

The applicability of this method was evaluated by analyzing six samples from a crossover station visited during the GEOTRACES GN04 Arctic Ocean cruise. Kipp et al. (2019) and

**Table 2.** Comparison between  $^{226}\text{Ra}$  measurement techniques in water samples.

Analytical method	Sample volume (L)	Detection limit (fg g <sup>-1</sup> )	Advantages	Disadvantages	References
ICP-MS	0.01–1	>0.002	Direct measurement of $^{226}\text{Ra}$ ; higher analytical precision; precise isotope ratio measurements; smaller sample size; short analytical time	Requires Ra purification; polyatomic and tailing interferences; sample matrix effects	Lagacé et al. (2017); Copia et al. (2015); Kim et al. (1999); Dalencourt et al. (2018); Yang et al. (2020); this study
Gamma spectrometry	1–1000	0.044–2.73	Four naturally-occurring radium isotopes analyzed simultaneously; low background levels; nondestructive technique; minimal sample preparation	Requires large volume samples. Low counting sensitivity; long waiting for ingrowth and counting times	Moore (1984); Cuttell et al. (1986); Parsa et al. (2004); Diab and Abdellah (2013); Medley et al. (2015)
Liquid scintillation spectroscopy (LSC)	1–4	0.009–0.541	High detection efficiency; relatively easy sample preparation; readily available LSC instrumentation	High background levels; long waiting for ingrowth and counting times	Burnett and Tai (1992); Tinker et al. (1995); Wallner and Steininger (2007)
Rn-emanation	1–20	0.156	High precision; low detection limit	Requires large volume samples; long waiting for ingrowth and counting times	Köhler et al. (2002)
Alpha spectrometry	0.1–20	0.003–0.547	High sensitivity. Low detection limit. No wait for ingrowth time	Requires complex chemical separation procedures and the use of a yield tracer	Rodríguez-Alvarez and Sánchez (1995); Baeza et al. (1998); Lawrie et al. (2000); Eikenberg et al. (2001)



Rutgers van der Loeff et al. (2018) reported  $^{226}\text{Ra}$  concentrations from the crossover station. The current results are in good agreement with their values. The current method takes approximately 3 d, comparable to the leaching procedure for gamma analysis. Eight to 10 samples could be prepared simultaneously, or more, depending on hot plates/stirrer availability. Measurement by mass spectrometry takes approximately 3 min per sample, so hundreds of samples can be analyzed per day (Table 1). In contrast, gamma spectrometry often requires 12–24 h measurement time per sample. Gamma spectrometry may also be unsuitable for low levels of Ra, and along with the Rn-emanation technique, requires waiting for  $^{222}\text{Rn}$  ingrowth if Ra is determined by its progenitors ( $^{214}\text{Pb}$  and  $^{214}\text{Bi}$ ). Table 2 summarizes the main features of the major techniques for  $^{226}\text{Ra}$  measurement.

This study provides a reliable method with an efficient Ra purification and analysis using a commonly available instrument. Thus, the proposed method provides an opportunity to measure  $^{226}\text{Ra}$  by ICP-MS easily and efficiently, which will ultimately contribute to its routine application.

### Comments and recommendations

The method described here showed an effective and reliable procedure for Ra purification and can be adapted to the investigation of Ra in other environmental matrices. Using the proposed method,  $^{226}\text{Ra}$  profiles of pore waters and sediments can be obtained, and concentrations in coral reefs, groundwater and freshwater can be determined. However, the concentration of Ba in these matrices is higher relative to seawater. The presence of Mg and Ca in groundwater, for example, may affect the sensitivity of HR-ICP-MS (Copia et al. 2015). Therefore, an additional column separation might be necessary (repeat column 1 or 2) to purify Ra in these matrices.

The element 2 instrument used in this study presents a special feature, which is an intermediate resolution of 2000 that can produce flat-top peaks, whereas the majority of the element 2 system provides analysis in low ( $R = 300$ ), medium ( $R = 4000$ ), and high ( $R = 10,000$ ) resolutions. However, the medium resolution (4000) does not provide flat-top peaks, and high resolution (10,000) has substantially reduced sensitivity. We recommend using medium resolution to check for interferences and the  $^{228}\text{Ra}/^{226}\text{Ra}$  ratios acquired in low resolution for the  $^{226}\text{Ra}$  determination by isotope dilution. This can be reliably performed with the current method given the successful reduction in interfering contaminants.

### References

Al-Hamarneh, I. F., and F. I. Almasoud. 2018. A comparative study of different radiometric methodologies for the determination of  $^{226}\text{Ra}$  in water. *Nucl. Eng. Technol.* **50**: 159–164. doi:10.1016/j.net.2017.10.009

- Baeza, A., L. M. Del Río, and A. Jiménez. 1998. Procedure for simultaneous determination of  $^{223,224,226,228}\text{Ra}$  by alpha and gamma spectrometry. *Radiochim. Acta* **83**: 53–60. doi:10.1524/ract.1998.83.2.53
- van Beek, P., M. Souhaut, and J. L. Reyss. 2010. Measuring the radium quartet ( $^{228}\text{Ra}$ ,  $^{226}\text{Ra}$ ,  $^{224}\text{Ra}$ ,  $^{223}\text{Ra}$ ) in seawater samples using gamma spectrometry. *J. Environ. Radioact.* **101**: 521–529. doi:10.1016/j.jenvrad.2009.12.002
- Bohlin, M. S., S. Misra, N. Lloyd, H. Elderfield, and M. J. Bickle. 2018. High-precision determination of lithium and magnesium isotopes utilising single column separation and multi-collector inductively coupled plasma mass spectrometry. *Rapid Commun. Mass Spectrom.* **32**: 93–104. doi:10.1002/rcm.8020
- Bourquin, M., P. van Beek, J. L. Reyss, J. Riotte, and R. Freydier. 2011. Determination of  $^{226}\text{Ra}$  concentrations in seawater and suspended particles (NW Pacific) using MC-ICP-MS. *Mar. Chem.* **126**: 132–138. doi:10.1016/j.marchem.2011.05.001
- Broecker, W. S., J. Goddard, and J. L. Sarmiento. 1976. The distribution of  $^{226}\text{Ra}$  in the Atlantic Ocean. *Earth Planet. Sci. Lett.* **32**: 220–235. doi:10.1016/0012-821X(76)90063-7
- Burnett, W. C., and W. C. Tai. 1992. Determination of radium in natural waters by  $\alpha$  liquid scintillation. *Anal. Chem.* **64**: 1691–1697. doi:10.1021/ac00039a012
- Burt, W. J., H. Thomas, J. Pätsch, A. M. Omar, C. Schrum, U. Daewel, H. Brenner, and H. J. W. Baar. 2014. Global biogeochemical cycles column exchange in the North Sea. *Global Biogeochem. Cycles* **28**: 786–804. doi:10.1002/2014GB004825
- Chabaux, F., D. Ben Othman, and J. L. Birck. 1994. A new Ra-Ba chromatographic separation and its application to Ra mass-spectrometric measurement in volcanic rocks. *Chem. Geol.* **114**: 191–197. doi:10.1016/0009-2541(94)90052-3
- Charette, M. A., and others. 2016. Coastal Ocean and shelf-sea biogeochemical cycling of trace elements and isotopes: Lessons learned from GEOTRACES. *Phil. Trans. R. Soc. A* **374**: 1–19.
- Charette, M. A., H. Dulaiova, M. E. Gonneea, P. B. Henderson, W. S. Moore, J. C. Scholten, and M. K. Pham. 2012. GEOTRACES radium isotopes interlaboratory comparison experiment. *Limnol. Oceanogr.: Methods* **10**: 451–463. doi:10.4319/lom.2012.10.451
- Chung, Y., and H. Craig. 1980. Ra-226 in the Pacific Ocean. *Earth Planet. Sci. Lett.* **49**: 267–292. doi:10.1016/0012-821X(80)90072-2
- Cohen, A. S., and R. K. O’Nions. 1991. Precise determination of femtogram quantities of radium by thermal ionization mass spectrometry. *Anal. Chem.* **63**: 2705–2708. doi:10.4135/9781446247501.n3887
- Copia, L., S. Nisi, W. Plastino, M. Ciarletti, and P. P. Povinec. 2015. Low-level  $^{226}\text{Ra}$  determination in groundwater by SF-ICP-MS: Optimization of separation and pre-concentration methods. *J. Anal. Sci. Technol.* **6**: 1–7. doi:10.1186/s40543-015-0062-5

- Cuttell, J. C., J. W. Lloyd, and M. Ivanovich. 1986. A study of uranium and thorium series isotopes in chalk groundwaters of Lincolnshire, UK. *J. Hydrol.* **86**: 343–365. doi:10.1016/0022-1694(86)90172-1
- Dalencourt, C., A. Michaud, A. Habibi, A. Leblanc, and D. Larivière. 2018. Rapid, versatile and sensitive method for the quantification of radium in environmental samples through cationic extraction and inductively coupled plasma mass spectrometry. *J. Anal. At. Spectrom* **33**: 1031–1040. doi:10.1039/c8ja00060c
- Diab, H. M., and W. M. Abdallah. 2013. Validation of Ra226 and Ra228 measurements in water samples using gamma spectrometric analysis. *J. Water Resour. Prot.* **05**: 53–57. doi:10.4236/jwarp.2013.58A008
- Diego-Feliu, M., and others. 2020. Guidelines and limits for the quantification of U/Th series radionuclides with the Radium Delayed Coincidence Counter (RaDeCC). *J. Geophys. Res. Ocean.* **125**: e2019JC015544. doi:10.1029/2019JC015544
- Eikenberg, J., A. Tricca, G. Vezzu, S. Bajo, M. Ruethi, and H. Surbeck. 2001. Determination of  $^{228}\text{Ra}$ ,  $^{226}\text{Ra}$  and  $^{224}\text{Ra}$  in natural water via adsorption on  $\text{MnO}_2$ -coated discs. *J. Environ. Radioact.* **54**: 109–131. doi:10.1016/S0265-931X(00)00170-3
- Epov, V. N., D. Lariviere, R. D. Evans, C. Li, and R. J. Cornett. 2003. Direct determination of  $^{226}\text{Ra}$  in environmental matrices using collision cell inductively coupled plasma mass-spectrometry. *J. Radioanal. Nucl. Chem.* **256**: 53–60. doi:10.1023/A:1023343824444
- Foster, D. A., M. Staubwasser, and G. M. Henderson. 2004.  $^{226}\text{Ra}$  and Ba concentrations in the Ross Sea measured with multicollector ICP mass spectrometry. *Mar. Chem.* **87**: 59–71. doi:10.1016/j.marchem.2004.02.003
- Garcia-Solsona, E., J. Garcia-Orellana, P. Masqué, and H. Dulaiova. 2008. Uncertainties associated with  $^{223}\text{Ra}$  and  $^{224}\text{Ra}$  measurements in water via a Delayed Coincidence Counter (RaDeCC). *Mar. Chem.* **109**: 198–219. doi:10.1016/j.marchem.2007.11.006
- Geibert, W., V. Rodellas, A. Annett, P. van Beek, J. Garcia-Orellana, Y.-T. Hsieh, and P. Masque. 2013.  $^{226}\text{Ra}$  determination via the rate of  $^{222}\text{Rn}$  ingrowth with the Radium Delayed Coincidence Counter (RaDeCC). *Limnol. Oceanogr.: Methods* **11**: 594–603. doi:10.4319/lom.2013.11.594
- Ghaleb, B., E. Pons-branchu, and P. Deschamps. 2004. Improved method for radium extraction from environmental samples and its analysis by thermal ionization mass spectrometry. *J. Anal. At. Spectrom* **19**: 906–910. doi:10.1039/b402237h
- Henderson, P. B., P. J. Morris, W. S. Moore, and M. A. Charette. 2013. Methodological advances for measuring low-level radium isotopes in seawater. *J. Radioanal. Nucl. Chem.* **296**: 357–362. doi:10.1007/s10967-012-2047-9
- Hou, X., and P. Roos. 2008. Critical comparison of radiometric and mass spectrometric methods for the determination of radionuclides in environmental, biological and nuclear waste samples. *Anal. Chim. Acta* **608**: 105–139. doi:10.1016/j.aca.2007.12.012
- Hsieh, Y. T., and G. M. Henderson. 2011. Precise measurement of  $^{228}\text{Ra}/^{226}\text{Ra}$  ratios and Ra concentrations in seawater samples by multi-collector ICP mass spectrometry. *J. Anal. At. Spectrom* **26**: 1338–1346. doi:10.1039/c1ja10013k
- Jia, G., and J. Jia. 2012. Determination of radium isotopes in environmental samples by gamma spectrometry, liquid scintillation counting and alpha spectrometry: A review of analytical methodology. *J. Environ. Radioact.* **106**: 98–119. doi:10.1016/j.jenvrad.2011.12.003
- Joannon, S., and C. Pin. 2001. Ultratrace determination of  $^{226}\text{Ra}$  in thermal waters by high sensitivity quadrupole ICP-mass spectrometry following selective extraction and concentration using radium-specific membrane disks. *J. Anal. At. Spectrom* **16**: 32–37.
- Key, R. M., N. L. Guinasso, and D. R. Schink. 1979. Emanation of radon-222 from marine sediments. *Mar. Chem.* **7**: 221–250.
- Kim, G., W. C. Burnett, H. Dulaiova, P. W. Swarzenski, and W. S. Moore. 2001. Measurement of  $^{224}\text{Ra}$  and  $^{226}\text{Ra}$  activities in natural waters using a radon-in-air monitor. *Environ. Sci. Technol.* **35**: 4680–4683. doi:10.1021/es010804u
- Kim, Y. J., C. K. Kim, C. S. Kim, J. Y. Yun, and B. H. Rho. 1999. Determination of  $^{226}\text{Ra}$  in environmental samples using high-resolution inductively coupled plasma mass spectrometry. *J. Radioanal. Nucl. Chem.* **240**: 613–618. doi:10.1007/BF02349421
- Kipp, L. E., D. C. Kadko, R. S. Pickart, P. B. Henderson, W. S. Moore, and M. A. Charette. 2019. Shelf-basin interactions and water mass residence times in the Western Arctic Ocean: Insights provided by radium isotopes. *J. Geophys. Res. Ocean.* **124**: 3279–3297. doi:10.1029/2019JC014988
- Knauss, K. G., T.-L. Ku, and W. S. Moore. 1978. Radium and thorium isotopes in the surface waters of the East Pacific and coastal Southern California. *Earth Planet. Sci. Lett.* **39**: 235–249.
- Köhler, M., W. Preuße, B. Gleisberg, I. Schäfer, T. Heinrich, and B. Knobus. 2002. Comparison of methods for the analysis of  $^{226}\text{Ra}$  in water samples. *Appl. Radiat. Isot.* **56**: 387–392. doi:10.1016/S0969-8043(01)00219-6
- Krishnaswami, S., and J. K. Cochran. 2008. U-Th series nuclides in aquatic systems. *Radioact. Environ.* **13**: 1–458. doi:10.1016/S1569-4860(07)00001-0
- Ku, T. L., and S. Luo. 2008. Ocean circulation/mixing studies with decay-series isotopes, p. 307–344. *In* J. K. Krishnaswami and S. Cochran [eds.], *Radioactivity in the environment*. Elsevier.
- Lagacé, F., D. Foucher, C. Surette, and O. Clarisse. 2017. Quantification of  $^{226}\text{Ra}$  at environmental relevant levels in natural waters by ICP-MS: Optimization, validation and limitations of an extraction and pre-concentration

- approach. *Talanta* **167**: 658–665. doi:[10.1016/j.talanta.2017.02.031](https://doi.org/10.1016/j.talanta.2017.02.031)
- Larivière, D., V. N. Epov, K. M. Reiber, R. J. Cornett, and R. D. Evans. 2005. Micro-extraction procedures for the determination of Ra-226 in well waters by SF-ICP-MS. *Anal. Chim. Acta* **528**: 175–182. doi:[10.1016/j.aca.2004.09.076](https://doi.org/10.1016/j.aca.2004.09.076)
- Lariviere, D., V. F. Taylor, R. D. Evans, and R. J. Cornett. 2006. Radionuclide determination in environmental samples by inductively coupled plasma mass spectrometry. *Spectrochim. Acta B At. Spectrosc.* **61**: 877–904. doi:[10.1016/j.sab.2006.07.004](https://doi.org/10.1016/j.sab.2006.07.004)
- Lawrie, W. C., J. A. Desmond, D. Spence, S. Anderson, and C. Edmondson. 2000. Determination of radium-226 in environmental and personal monitoring samples. *Appl. Radiat. Isot.* **53**: 133–137. doi:[10.1016/S0969-8043\(00\)00168-8](https://doi.org/10.1016/S0969-8043(00)00168-8)
- Leermakers, M., Y. Gao, J. Navez, A. Poffijn, K. Croes, and W. Baeyens. 2009. Radium analysis by sector field ICP-MS in combination with the diffusive gradients in thin films (DGT) technique. *J. Anal. At. Spectrom.* **24**: 1115–1117. doi:[10.1039/b821472g](https://doi.org/10.1039/b821472g)
- Medley, P., P. Martin, A. Bollhöfer, and D. Parry. 2015.  $^{228}\text{Ra}$  and  $^{226}\text{Ra}$  measurement on a  $\text{BaSO}_4$  co-precipitation source. *Appl. Radiat. Isot.* **95**: 200–207. doi:[10.1016/j.apradiso.2014.09.015](https://doi.org/10.1016/j.apradiso.2014.09.015)
- Michel, J., W. S. Moore, and P. T. King. 1981.  $\gamma$ -Ray spectrometry for determination of radium-228 and radium-226 in natural waters. *Anal. Chem.* **53**: 1885–1889. doi:[10.1021/ac00235a038](https://doi.org/10.1021/ac00235a038)
- Moon, D. S., W. C. Burnett, S. Nour, P. Horwitz, and A. Bond. 2003. Preconcentration of radium isotopes from natural waters using  $\text{MnO}_2$  resin. *Appl. Radiat. Isot.* **59**: 255–262. doi:[10.1016/S0969-8043\(03\)00193-3](https://doi.org/10.1016/S0969-8043(03)00193-3)
- Moore, W. S. 1969. Oceanic concentrations of  $^{228}\text{Ra}$ . *Earth Planet. Sci. Lett.* **6**: 437–446. doi:[10.1016/0012-821X\(69\)90113-7](https://doi.org/10.1016/0012-821X(69)90113-7)
- Moore, W. S. 1984. Radium isotope measurements using germanium detectors. *Nucl. Instrum. Methods Phys. Res.* **223**: 407–411. doi:[10.1016/0167-5087\(84\)90683-5](https://doi.org/10.1016/0167-5087(84)90683-5)
- Moore, W. S. 2008. Fifteen years experience in measuring  $^{224}\text{Ra}$  and  $^{223}\text{Ra}$  by delayed-coincidence counting. *Mar. Chem.* **109**: 188–197. doi:[10.1016/j.marchem.2007.06.015](https://doi.org/10.1016/j.marchem.2007.06.015)
- Moore, W. S., and R. Arnold. 1996. Measurement of  $^{223}\text{Ra}$  and  $^{224}\text{Ra}$  in coastal waters using a delayed coincidence counter. *J. Geophys. Res.* **101**: 1321–1329. doi:[10.1029/95jc03139](https://doi.org/10.1029/95jc03139)
- Moore, W. S., M. Beck, T. Riedel, M. M. Rutgers van der Loeff, O. Dellwig, T. J. Shaw, B. Schnetger, and H. J. Brumsack. 2011. Radium-based pore water fluxes of silica, alkalinity, manganese, DOC, and uranium: A decade of studies in the German Wadden Sea. *Geochim. Cosmochim. Acta* **75**: 6535–6555. doi:[10.1016/j.gca.2011.08.037](https://doi.org/10.1016/j.gca.2011.08.037)
- Moore, W. S., and J. Dymond. 1991. Fluxes of  $^{226}\text{Ra}$  and barium in the Pacific Ocean: The importance of boundary processes. *Earth Planet. Sci. Lett.* **107**: 55–68. doi:[10.1016/0012-821X\(91\)90043-H](https://doi.org/10.1016/0012-821X(91)90043-H)
- Nelson, A. W., D. May, A. W. Knight, E. S. Eitheim, M. Mehrhoff, R. Shannon, R. Litman, and M. K. Schultz. 2014. Matrix complications in the determination of radium levels in hydraulic fracturing flowback water from marcellus shale. *Environ. Sci. Technol. Lett.* **1**: 204–208. doi:[10.1021/ez5000379](https://doi.org/10.1021/ez5000379)
- Ollivier, P., C. Claude, O. Radakovitch, and B. Hamelin. 2008. TIMS measurements of  $^{226}\text{Ra}$  and  $^{228}\text{Ra}$  in the Gulf of Lion, an attempt to quantify submarine groundwater discharge. *Mar. Chem.* **109**: 337–354. doi:[10.1016/j.marchem.2007.08.006](https://doi.org/10.1016/j.marchem.2007.08.006)
- Park, C. J., P. J. Oh, H. Y. Kim, and D. S. Lee. 1999. Determination of  $^{226}\text{Ra}$  in mineral waters by high-resolution inductively coupled plasma mass spectrometry after sample preparation by cation exchange. *J. Anal. At. Spectrom.* **14**: 223–227. doi:[10.1039/a808234k](https://doi.org/10.1039/a808234k)
- Parsa, B., R. N. Obed, W. K. Nemeth, and G. Suozzo. 2004. Concurrent determination of  $^{224}\text{Ra}$ ,  $^{226}\text{Ra}$ ,  $^{228}\text{Ra}$ , and unsupported  $^{212}\text{Pb}$  in a single analysis for drinking water and wastewater: Dissolved and suspended fractions. *Health Phys.* **86**: 145–149. doi:[10.1097/00004032-200402000-00004](https://doi.org/10.1097/00004032-200402000-00004)
- Reyss, J. L., S. Schmidt, F. Legeleux, and P. Bonté. 1995. Large, low background well-type detectors for measurements of environmental radioactivity. *Nucl. Inst. Methods Phys. Res. A* **357**: 391–397. doi:[10.1016/0168-9002\(95\)00021-6](https://doi.org/10.1016/0168-9002(95)00021-6)
- Rodríguez-Alvarez, M. J., and F. Sánchez. 1995. Measurement of radium and thorium isotopes in environmental samples by alpha-spectrometry. *J. Radioanal. Nucl. Chem. Artic.* **191**: 3–13. doi:[10.1007/BF02035979](https://doi.org/10.1007/BF02035979)
- Roy, E., and others. 2018. The  $^{226}\text{Ra}$ -Ba relationship in the North Atlantic during GEOTRACES-GA01. *Biogeosciences* **15**: 3027–3048.
- Rutgers van der Loeff, M., and others. 2018. Radium isotopes across the Arctic Ocean show time scales of water mass ventilation and increasing shelf inputs. *J. Geophys. Res. Ocean.* **123**: 4853–4873. doi:[10.1029/2018JC013888](https://doi.org/10.1029/2018JC013888)
- Sanial, V., and others. 2018. Radium-228 as a tracer of dissolved trace element inputs from the Peruvian continental margin. *Mar. Chem.* **201**: 20–34. doi:[10.1016/j.marchem.2017.05.008](https://doi.org/10.1016/j.marchem.2017.05.008)
- Schmidt, C., C. Hanfland, P. Regnier, P. van Cappellen, M. Schlüter, U. Knauthe, I. Stimac, and W. Geibert. 2011.  $^{228}\text{Ra}$ ,  $^{226}\text{Ra}$ ,  $^{224}\text{Ra}$  and  $^{223}\text{Ra}$  in potential sources and sinks of land-derived material in the German Bight of the North Sea: Implications for the use of radium as a tracer. *Geo-Marine Lett.* **31**: 259–269. doi:[10.1007/s00367-011-0231-5](https://doi.org/10.1007/s00367-011-0231-5)
- Sharabi, G., B. Lazar, Y. Kolodny, N. Teplyakov, and L. Halicz. 2010. High precision determination of  $^{228}\text{Ra}$  and  $^{228}\text{Ra}/^{226}\text{Ra}$  isotope ratio in natural waters by MC-ICPMS. *Int. J. Mass Spectrom.* **294**: 112–115. doi:[10.1016/j.ijms.2010.05.011](https://doi.org/10.1016/j.ijms.2010.05.011)
- Strelow, F. W. E. 1984. Distribution coefficients and ion exchange behavior of 46 elements with a macroreticular

- cation exchange resin in hydrochloric acid. *Anal. Chem.* **56**: 1053–1056. doi:10.1021/ac00270a045
- Thakur, P., A. L. Ward, and A. M. González-Delgado. 2021. Optimal methods for preparation, separation, and determination of radium isotopes in environmental and biological samples. *J. Environ. Radioact.* **228**: 106522. doi:10.1016/j.jenvrad.2020.106522
- Tinker, R. A., J. D. Smith, and M. B. Cooper. 1995. An assessment of the selection criteria for an analytical method for radium-226 in environmental samples. *J. Radioanal. Nucl. Chem.* **193**: 329–336.
- Varga, Z. 2008. Ultratrace-level radium-226 determination in seawater samples by isotope dilution inductively coupled plasma mass spectrometry. *Anal. Bioanal. Chem.* **390**: 511–519. doi:10.1007/s00216-007-1394-9
- Verlinde, M., and others. 2019. A new rapid protocol for  $^{226}\text{Ra}$  separation and preconcentration in natural water samples using molecular recognition technology for ICP-MS analysis. *J. Environ. Radioact.* **202**: 1–7. doi:10.1016/j.jenvrad.2019.02.003
- Vernet, M., and others. 2019. The Weddell Gyre, Southern Ocean: Present knowledge and future challenges. *Rev. Geophys.* **57**: 623–708. doi:10.1029/2018RG000604
- Wallner, G., and G. Steininger. 2007. Radium isotopes and  $^{222}\text{Rn}$  in Austrian drinking waters. *J. Radioanal. Nucl. Chem.* **274**: 511–516. doi:10.1007/s10967-006-6939-4
- Waska, H., S. Kim, G. Kim, R. N. Peterson, and W. C. Burnett. 2008. An efficient and simple method for measuring  $^{226}\text{Ra}$  using the scintillation cell in a delayed coincidence counting system (RaDeCC). *J. Environ. Radioact.* **99**: 1859–1862. doi:10.1016/j.jenvrad.2008.08.008
- Yang, G., J. Zheng, K. Tagami, S. Uchida, J. Zhang, J. Wang, and J. Du. 2020. Simple and sensitive determination of radium-226 in river water by single column-chromatographic separation coupled to SF-ICP-MS analysis in medium resolution mode. *J. Environ. Radioact.* **220–221**: 106305. doi:10.1016/j.jenvrad.2020.106305
- Zoriy, M. V., Z. Varga, C. Pickhardt, P. Ostapczuk, R. Hille, L. Halicz, I. Segal, and J. S. Becker. 2005. Determination of  $^{226}\text{Ra}$  at ultratrace level in mineral water samples by sector field inductively coupled plasma mass spectrometry. *J. Environ. Monit.* **7**: 514–518. doi:10.1039/b503011k

### Acknowledgment

We acknowledge funding from the Helmholtz Association via the Network of Excellence “The Polar System and its Effects on the Ocean Floor (POSY)” (ExNet-0001). Open access funding enabled and organized by Projekt DEAL.

Submitted 02 November 2020

Revised 25 February 2021

Accepted 07 March 2021

Associate editor: Isaac Santos